IET Nanobiotechnology

Research Article

IET Journals
The Institution of Engineering and Technology

ISSN 1751-8741
Received on 17th October 2017
Revised 19th April 2018
Accepted on 20th June 2018
E-First on 26th September 2018
doi: 10.1049/iet-nbt.2018.5052
www.ietdl.org

Effect of chitosan with different molecular weight on the stability, antioxidant and anticancer activities of well-dispersed selenium nanoparticles

Wanwen Chen[1], Lin Yue[1], Qixing Jiang[1], Wenshui Xia[1] ✉

[1]*State Key Laboratory of Food Science and Technology, School of Food Science and Technology, Collaborative Innovation Center of Food Safety and Quality Control in Jiangsu Province, Jiangnan University, Lihu Road 1800, Wuxi, 214122 Jiangsu, People's Republic of China*

✉ *E-mail: xiaws@jiangnan.edu.cn*

Abstract: This study was designed to evaluate and compare the stability, antioxidant and anticancer activities of selenium nanoparticles (SeNPs) decorated with different molecular weight (MW) of chitosan (CS) (1500 Da, 48 kDa, 510 kDa). The size range of well-dispersed SeNPs was effectively controlled by I^- first and then coated with CS. The morphology, size and surface charge of generated SeNPs were characterised by several technologies. Fourier transform infrared spectroscopy was used to investigate the relationship between SeNPs and CS. SeNPs decorated with CS (510 kDa) can keep stable for more than 45 days. As observed from the results of a simple photometric system, the antioxidant activities of decorated SeNPs were enhanced compared to undecorated SeNPs. SeNPs coated with higher MW of CS (510 kDa) showed the strongest antioxidant activities. Moreover, the treatments of SeNPs decorated with CS inhibited the growth of HepG2 cells in a time- and dose-dependent manner. The proposed results demonstrated the critical roles of the MW of CS on the stability, antioxidant and anticancer properties of CS-coated SeNPs, which provided an important design cue for future applications of functional foods and additives.

1 Introduction

During the last few years, there has been a growing interest to develop materials with high antioxidant and antimicrobial properties which help to improve the quality of food, enhance the shelf life and ensure the safety of food [1]. Nanotechnology is a highly promising interdisciplinary technology that spans across food, material and biomedical areas with the development of new nanoparticles, which have unique biological properties enable them to bind, absorb and carry compounds such as small molecule drugs, DNA, RNA, proteins and probes with high efficiency [2]. The compositions, structure and charge of NPs vary via different fabrication methods, which may affect the stability and antioxidant properties [3].

The essential trace element, selenium, is of vital importance to human health. Selenium exerts its biological function through several selenoproteins, including a number of glutathione peroxidases (GPx) [4]. It is involved in the complex system of defence against oxidative stress functions in the body as an antioxidant, in thyroid hormone metabolism, redox reactions, reproduction and immune function. The dose and form of selenium are the determining factors related to its biological activity, toxicity and cancer prevention [5]. SeNPs are novel selenium species with unique biological, appearing to be more effective than other forms of selenium at increasing selenoproteins expression, scavenging free radicals, and preventing oxidative DNA damage as antioxidant [6, 7]. SeNPs also have additional benefits such as low toxicity and acceptable bioavailability, which have aroused widespread attention in recent years [8–10]. Since SeNPs have drawbacks that are prone to aggregation without controlling factors, leading to lower bioactivity and restricting its application, mounting evidences suggested that nature polymers, such as some polysaccharides, proteins and vitamins, which seemed to be either non-toxic, biocompatible and biodegradable are used as stabiliser to fabricate SeNPs for food and biomedical applications. These polymers can not only control the size and stability of SeNPs but also enhance bioactivity, including anti-oxidation, anti-viral activities, immune regulation, anti-oncological activity and anti-ageing effects. Folic acid modified selenium nanoparticles (SeNPs) could be served as potential therapeutic agents and organelle-targeted drug carriers in cancer therapy [11]. Polysaccharide protein complexes SeNPs are potential chemopreventive agents for lung cancer therapy [12]. SeNPs decorated with polysaccharides–protein complexes exhibited higher antiproliferative activity, compared with undecorated SeNPs [13].

Chitosan (CS) is the N-deacetylated derivative of chitin, regarded as the only pseudonatural cationic polymer in the world, which mainly obtained from the cell walls of fungal and yeast and the shell of krill, lobster and crab. It also has good biodegradability and excellent bioactivities such as antioxidant, antitumor, so it is a candidate to disperse and stabilise SeNPs. According to previous studies, Yu introduced CS to synthesise SeNPs with the large size about 120 nm, which may not be controllable to synthesise smaller size of NPs [14]. Zhang had employed different molecular weight (MW) of CS to stabilise SeNPs and investigated the stability and antioxidant activities, they used CS as capping agent during the synthesis of SeNPs, while SeNPs decorated with high MW of CS were aggregated markedly and SeNPs stabilised with low MW of CS were dispersed well with amount of 20–50 nm aggregates. The size and morphology of NPs were uncontrollable and the effect of different MW of CS on SeNPs was elusive, due to that CS has a key role in the reducing reaction. Moreover, they just investigated the antioxidant properties of decorated CS during storage at 0 day and 30 days, while no comparison was focused on the difference of antioxidant and anticancer properties between SeNPs coated with different MW of CS [15, 16]. Though little studies that have been performed using CS as stabiliser to synthesise SeNPs, it remains unclear the difference between the different MW of CS coated SeNPs on the antioxidant and anticancer activities. Our previous work suggested that well-dispersed SeNPs decorated with polysaccharide of opposite surface charge (CS, carboxymethyl chitosan) were potent antioxidants in vitro. Recently, several works have focused on the roles of I^- on the synthesis of nanocrystals which performed as reactant and surface stabilising agent, thereby reducing the complexity of the synthesis by eliminating the need for an external capping agent [17]. In this study, SeNPs were

synthesised using I^- as capping agent first and different MW of CS were anchored on the monodisperse SeNPs. Coupled with the desired biomolecules, these stable decorated SeNPs should have great potentials for biomedical applications in food systems. To the best of our knowledge and according to a survey of the literature, there is no report to investigate the difference on the stability, antioxidant and anticancer activities of the different MW of CS decorated SeNPs systematically.

2 Materials and methods

2.1 Materials

The CS with a MW of 510 kDa (CS(h)), 48 kDa (CS(m)) and 1500 Da (CS(l))(Poly-β-(1,4)-D-glucosamine with 95% degree of deacetylation) were obtained from our own lab. Dulbecco's modified Eagle's medium (DMEM) and foetal bovine serum (FBS) and 4–3-(4-Iodophenyl)-2-(4-Nitrophenyl)-2H-5-Tetrazolio]-1,3-Benzene Disulfonate (WST-1), penicillin and streptomycin were purchased from NEST Co. All other chemical reagents were of analytical grade. All water used in the analysis had been distilled and deionised.

2.2 Synthesis of different MW of CS-SeNPs

In order to obtain SeNPs, we considered the method described in our previous work with some modification. About 20 mM Na_2SeO_3 aqueous solution was mixed with 30 mM KI under magnetic stirring. Then 60 mM freshly prepared ascorbic acid solution was added then dropwise into the mixture and stirred for 30 min at the room temperature. The resulting colloid was aged for 24 h and purified by dialysis overnight against ultrapure water in a dialysis bag (500 g/mol MW cut off from Mym Biological Technology Company) with constant stirring to eliminate interferences from Vc and KI. CS (1500 Da, 48 kDa, 510 kDa) with different concentrations (0.08, 0.16, 0.32, 0.48, 0.64 mg/ml) were added into the SeNPs colloidal to obtain CS (l)-SeNPs, CS (m)-SeNPs, CS (h)-SeNPs. The final solution was stored at 4°C for further use.

2.3 Characterisation and measurements

Several methods were used to characterise the synthesised nanoparticles. Transmission electron microscopy (TEM, JEOL JEM-2100, Japan) was performed to characterise the size and morphology of SeNPs. UV–visible spectra were recorded on the Shimadzu UV-1800 spectrometer. The size distribution of the nanoparticles was measured by Zetasizer Nano ZS instrument (Malvern Instruments Limited). Fourier transform infrared (FTIR) spectra were obtained with Nicolet iS 10 instrument using potassium bromide pellets within the range of 400–4000 cm^{-1}. Mettler Toledo TGA/SDTA851 thermogravimeter was used to obtain thermogravimetric analysis curves under the temperature range of 30–550°C.

2.4 Assay for antioxidant activities

2.4.1 DPPH radical scavenging activity: The free radical scavenging activities of SeNPs, CS(l)-SeNPs, CS(m)-SeNPs and CS(h)-SeNPs on DPPH radical were investigated by DPPH test employing the method [18] with some modifications. Briefly, 5 ml of sample solution with different concentration (0.1–0.5 mM SeNPs added with the same concentration of 0.08 mg/ml different MW of CS) was mixed with 5 ml DPPH ethanol solution (50 mg/l). The mixture was incubated for 30 min at 33°C. The absorbance was then measured at 517 nm. Lower values of absorbance mean a higher DPPH scavenging activity. The DPPH radical scavenging ability was calculated as follows:

$$\text{DPPH radical scavenging ability}(\%) = (A_c - A_a + A_b)/A_c \times 100 \quad (1)$$

where A_c is the absorbance of DPPH without sample, A_a is the absorbance of the sample mixed with DPPH solution, A_b is the absorbance of the sample without DPPH solution.

2.4.2 ABTS radical cation scavenging activity: In-vitro antioxidant activity towards $ABTS^{\bullet+}$ was evaluated according to the method [19] with some modification. In this method, 7.4 mM ABTS was mixed with $K_2S_2O_8$ to generate $ABTS^{\bullet+}$. A stable oxidation was formed until reacted for all night in the dark. Then the mixture was diluted with ethanol to give an absorbance of 0.700 ± 0.01 at 734 nm. About 40 µl of different samples at different concentrations (0.1–2.0 mM SeNPs added with the same concentration of 0.08 mg/ml different MW of CS) was added with 160 µl of $ABTS^{\bullet+}$ solution and reacted for 6 min in a dark condition. The absorbance of the resulting solution was measured at 734 nm using ELIASA. The scavenging ability was calculated using the following formula:

$$\text{ABTS}^{\cdot+}\text{ radical scavenging ability}(\%) = (A_c - A_a + A_b)/A_c \times 100 \quad (2)$$

where A_c is the absorbance of a control, A_a is the absorbance of sample and reagent, A_b is the absorbance of the sample without reagent.

2.4.3 Superoxide anion radical scavenging activity: The influence of SeNPs on the generation of superoxide was measured by means of spectrophotometric measurement with some modification [8]. The 50 mM Tris-HCl buffer (pH 8.2) have been incubated at 25°C for 20 min, then 1 ml of samples solution at various concentrations (0.2–1 mM SeNPs added with the same concentration of 0.08 mg/ml different MW of CS) and 3 mM pyrogallic acid were added and rapidly shaken. The resulting mixture was incubated for 5 min at 25°C in the dark. Thereafter, 10 mM HCl was added to terminate the reaction, and the absorbance was measured at 320 nm. The ability to scavenge $O_2^{\bullet-}$ was calculated as follows:

$$O_2^{\cdot-}\text{ radical scavenging ability}(\%) = (A_c - A_a + A_b)/A_c \times 100 \quad (3)$$

where A_a is the absorbance of sample and reagent and A_b is absorbance of the sample without $O_2^{\bullet-}$, while A_c is absorbance of a control (blank).

2.5 Cell culture

HepG2 was maintained at 1×10^6 cells/ml in DMEM media supplemented with FBS (10%), penicillin (100 units/ml) and streptomycin (50 units/ml) at 37°C in CO_2 incubator (95% relative humidity, 5% CO_2). The morphology of the cells was observed under an inverted microscope (Nikon, Japan).

2.6 Cytotoxicity assay

Cytotoxicity of SeNPs, CS(l)-SeNPs, CS(m)-SeNPs and CS(h)-SeNPs towards HepG2 cells was evaluated by the WST-1 [4–3-(4-Iodophenyl)-2-(4-Nitrophenyl)-2H-5-Tetrazolio]-1,3-Benzene Disulfonate] colorimetric assay based on the conversion of stable tetrazolium to a soluble formazan by a complex cellular mechanism that occurs primarily at the cell surface [20]. In starting experiments, each cell line was seeded at 5×10^4 cells/ml in a 96-well plate and cells were allowed to settle overnight. Cells were treated for 48 h with samples in different concentrations of 10, 50, 100 µM. At the end of the cultivation period, the WST-1 proliferation assay was performed according to the manufacturer's protocol and the absorbance was measured at 450 nm. The percentage of cell viability and the percentage of inhibition at various concentrations were calculated using the following formulae:

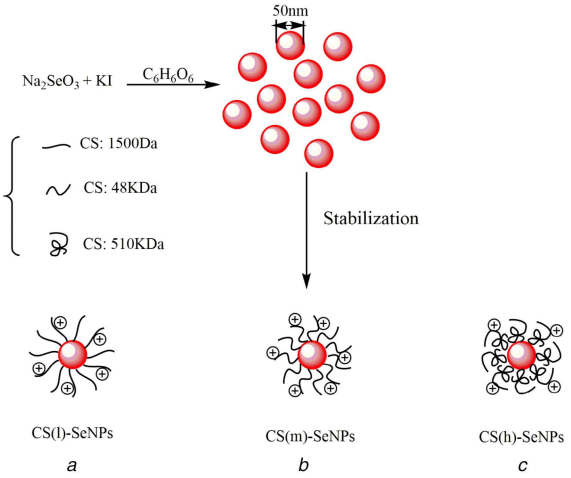

Fig. 1 *Symbolic illustraton of*
(a) CS(l)-SeNPs nanoparticles, ***(b)*** CS(m)-SeNPs nanoparticles, ***(c)*** CS(h)-SeNPs nanoparticles. NPs in (a), (b) and (c) are coated with CS of different MW

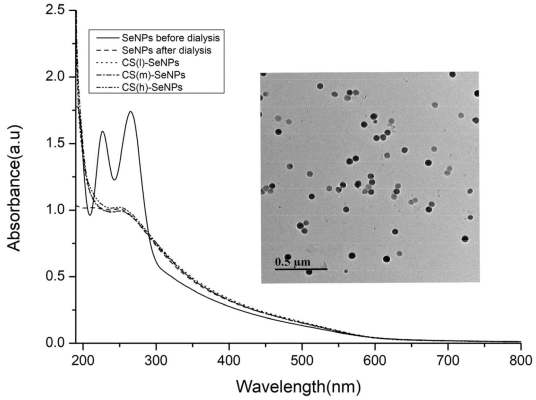

Fig. 2 *UV–Vis spectra of SeNPs before dialysis, SeNPs before dialysis, CS(l)-SeNPs, CS(m)-SeNPs, CS(h)-SeNPs and representative TEM image (inset) of SeNPs. The scale bar of the inset corresponds to 500 nm*

$$\text{Cell viability}\,(\%) = A_t/A_c \times 100 \tag{4}$$

where A_t is the absorbance of the test sample and A_c is the absorbance of the control.

3 Results and discussion

3.1 Formation and morphology of SeNPs coated with CS

In our experiments, well-dispersed SeNPs are first prepared by reducing Na_2SeO_3 with ascorbic acid in the presence of KI. According to previous studies, the ability of I^- to act as a surface regulating agent has been reported, such as to generate CuI nanoterahedrons [21], β-AgI [22] and it is believed that it forms a double layer between the surface adsorbed I^- and the counter ions (Na^+ or K^+), which generates a repulsive interaction between NPs to against aggregation. In order to clearly investigate the effect of different MW of CS decorated on SeNPs, we chose SeNPs with uniformity of the particle size distribution, surface-modified with different CS chain lengths of either 1500 Da, 48 kDa or 510 kDa on the top of polymer shell; the mechanism is shown in Fig. 1.

Addition of ascorbic acid to sodium selenite solution led to the appearance of an orange colour in solution, after about ageing 24 h, it turned to brownish red, which indicated the formation of SeNPs. The UV–Vis absorption spectra recorded from this solution showed the characteristic band of SeNPs. As shown in Fig. 2, the characteristic absorbance peak of SeNPs and decorated SeNPs exhibited the same position located at 253 nm. As shown in Fig. 2, SeNPs before dialysis exhibited two strong peaks at 226 and 265 nm, respectively, which represented the characteristic absorptions of potassium iodide and ascorbic acid. It was important to point out that there were no these peaks occurred in the whole spectrum, which indicated that the samples were purified via dialysis. As shown in the representative TEM image (insert) in Fig. 2, the synthesised SeNPs were well-dispersed spherical particles controlled by KI with the average diameter about 50 nm. The addition of CS did not change the morphology of SeNPs. According to Zhang's study, SeNPs stabilised by low MW CS showed a small amount of 20–50 nm aggregates. While, most of SeNPs dispersed in high MW CS were markedly aggregated [15]. Thereafter, in our paper, the decoration of different weight of CS on the well-dispersed SeNPs did not change the particle size.

3.2 DLS analysis

Stability of nanomaterials is an important factor that affects its application in food and pharmaceutical industry. The size distribution and stability of CS-SeNPs were investigated by a Zetasizer Nano-ZS particle analyser. In order to study the influence of CS surface density, nanoparticles were decorated with increased CS concentration. As shown in Fig. 3*a*, the SeNPs without CS showed an average size of 102.60 nm. Diameters of CS (l)-SeNPs were detected to be 102.95, 103.25, 103.35, 103.70, 104.35 nm when decorated with CS at concentration of 0.08, 0.16, 0.32, 0.48, 0.64 mg/ml, respectively. Diameters of CS (m)-SeNPs were determined by DLS to be 109.40, 111.15, 113.80, 119.90, 135.30 nm and the average size of CS (h)-SeNPs were about 124.55, 143.60, 152.55, 167.45, 182.40 nm at the same serious of concentrations of CS (l), which showed that by using different concentrations of CS as capping agent, the average particles size of CS-SeNPs was effectively increased as the concentration of CS increased, it may due to that with the concentration increased, the molecular spacing decreased, intermolecular hydrogen bond force enhanced, which resulted in the more crosslinking between MW. We could observe that the changes of size distribution of CS (m)-SeNPs was greater than CS (l)-SeNPs and lower than CS (h)-SeNPs, which might be due to the difference of MW of CS. With the same concentration, the bigger the MW of CS, the more packages in the surface of the SeNPs, which resulted in the larger particle size. As we know, recommended values of zeta potential for colloid suspension must have values superior to ±30 mV, which showed higher stability [23]. As shown in Fig. 3*b*, zeta potential value of SeNPs was about −28.4 mV. As we know that CS is the only positively charged natural polysaccharide in the world, due to that CS has many protonated amino group under acid conditions, which shows positive charge. Therefore, the zeta potential values for CS (l)-SeNPs, CS (m)-SeNPs, CS (h)-SeNPs were about +33.6, +48.35 and +63.05 mV at the concentration of 0.64 mg/ml, which could be seen that the CS-SeNPs exhibited a positive charge on the surface, while SeNPs showed negative charge. It should be pointed out that the stability of CS (l)-SeNPs may not as good as CS (m)-SeNPs and CS (h)-SeNPs. It may be due to that under the same concentration, the higher the CS MW, the bigger surface density surround the SeNPs, which may result in its stability. Besides, the stability of CS coated SeNPs were detected by monitoring the change in zeta potential during 45 days storage. As shown in Fig. 3*c*, the zeta potential of SeNPs with high and middle MW CS was much higher than SeNPs with low MW, it kept almost constant vales for 5 days, but both exhibited a slight decrease with one month or more time storage, which meant that CS (m)-SeNPs and CS (h)-SeNPs can keep stable for a month more than CS (l)-SeNPs.

3.3 FTIR analysis

In order to clarify the interaction between SeNPs and different MWs of CS, the FTIR spectra were collected as shown in Fig. 4. The FTIR spectra of CS (l) (MW = 1500 Da) exhibited main absorption bands at 3425.79 (O–H stretch), 2926.27 (C–H stretch), 1629.16 (C=O stretch, amide I), 1512.54 (N–H bend, amide II), 1382.46 (C–N stretch), 1087.77 cm^{-1} (C–O stretch). Compared to spectrum of CS (l), the characteristic peak of O–H group in CS (l)-SeNPs at 3401.98 cm^{-1} showed a blue shift, which indicated that CS (l) was conjugated to the surface of SeNPs through –OH group.

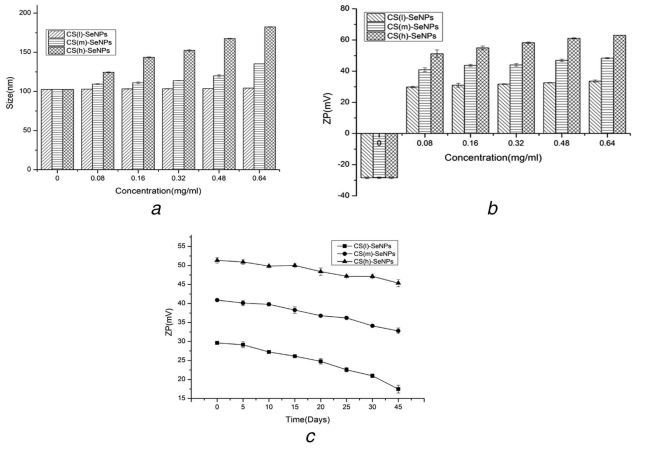

Fig. 3 *The DLS analysis of CS(l)-SeNPs, CS(m)-SeNPs, CS(h)-SeNPs*
(a) Particle size distribution, ***(b)*** Zeta potential distribution with increased CS concentration, ***(c)*** Zeta potential variation during 45 days storage

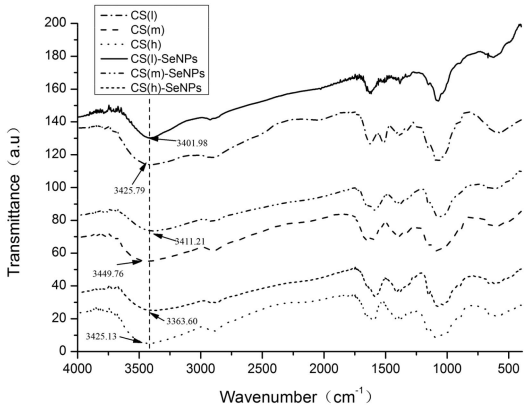

Fig. 4 *FTIR spectra of SeNPs decorated with different MWs of CS*

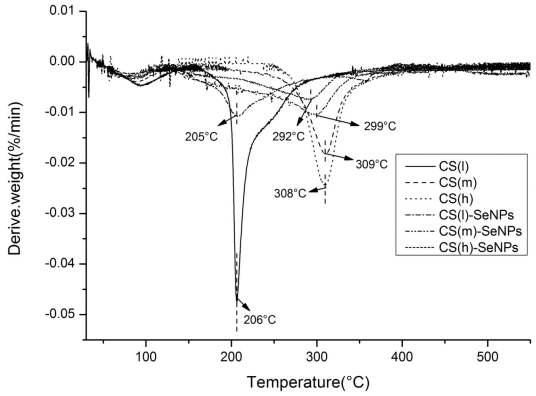

Fig. 5 *Thermogravimetric curves of CS(l), CS(m), CS(h), CS(l)-SeNPs, CS(m)-SeNPs and CS(h)-SeNPs*

Similarly, the characteristic peak of O–H group on CS (m)-SeNPs and CS (h)-SeNPs were also exhibited a blue-shift compared to CS (m) and CS (h). Taken together, the FTIR spectra supported that the OH groups of CS bound to the surface of SeNPs, which created a stable microenvironment for SeNPs in order to protect it from further accumulation.

3.4 Thermogravimetric analysis

Thermogravimetry is widely used to detect the thermal properties of materials. As shown in Fig. 5, the maximum degradation temperature (T_{max}) of CS(l), CS(m), CS(h) were at about 206, 309, 308°C, respectively, while the SeNPs coated with different MW CS, the CS(l)-SeNPs, CS(m)-SeNPs and CS(h)-SeNPs had T_{max} around 205, 299 and 292°C, which were similar to CS(l), CS(m), CS(h), but still exhibited a slight decrease. According to previous studies, the T_{max} value of SeNPs was about 409°C, it showed much higher thermal stabilities than CS-SeNPs. It may due to that CS is a polysaccharide, which is unstable at high temperature and the colour become deep. Therefore, SeNPs coated with CS may decompose more easily compared to SeNPs.

3.5 DPPH radical scavenging ability

The relatively stable DPPH radicals are nitrogen-centred and lipophilic-free radical, which can be reduced to a yellow-coloured compound as diphenylpicryl hydrazine in the presence of antioxidants [24], and the reaction involved H-atom transfer. It has been widely used to test the antioxidant ability of compounds to act as free radical scavengers. According to previous studies, some researchers indicated that SeNPs exhibited strong DPPH radical scavenging abilities [25, 26]. As shown in Fig. 6*a*, ascorbic acid was investigated as a positive contrast, the scavenging activity of SeNPs, CS(l)-SeNPs, CS(m)-SeNPs, CS(h)-SeNP on DPPH radicals investigated, which was significantly higher than inorganic selenium. The scavenging rate increased with increasing concentration. More importantly, SeNPs decorated with CS all showed excellent antioxidant activities to DPPH radicals compared to SeNPs at all concentration range, the scavenging abilities of SeNPs coated with different MW CS were close at the low concentration, while above 0.3 mM, the of CS (m)-SeNPs was lower than CS (h)-SeNP, but higher than CS (l)-SeNPs. Therefore, CS (h)-SeNP showed the best scavenging ability, which reached 83.06% at the concentration of 0.5 mM. Moreover, the IC_{50} values of SeNPs, CS(l)-SeNPs, CS(m)-SeNPs, CS(h)-SeNP were 0.370, 0.325, 0.306 and 0.296 mM, respectively. This may be due to that the mechanism of scavenging activity is related to the fact that residual free amino groups of CS can react with the free radicals, and the NH_2 groups can absorb a hydrogen ion to form ammonium (NH_3^+) groups while the extent of the reaction depends on the hydrogen-donating ability of the antioxidants. Therefore, at the same concentration, the higher MW of CS may contain more NH_2 groups, so that CS (h)-SeNP showed the higher scavenging abilities.

3.6 ABTS radical cation scavenging ability

$ABTS^{\bullet+}$ radicals are generated by oxidation of ABTS with potassium persulphate and involve an electron-transfer process, which are more reactive [27]. As seen in Fig. 6*b*, obvious concentration-dependent manner of SeNPs and CS-SeNPs on scavenging $ABTS^{\bullet+}$ was observed in the concentration range of 0.1–2 mM. CS(h)-SeNPs showed a strong ABTS scavenging ability than SeNPs on the whole, while no obvious difference was found between the SeNPs and CS(l)-SeNPs. It should be pointed out that CS(l)-SeNPs, CS(m)-SeNPs, CS(h)-SeNPs exhibited a higher ABTS scavenging ability which reached 74.33, 80.23 and 81.99% at a concentration of 2 mmol/l, respectively. The IC_{50} values of SeNPs, CS(l)-SeNPs, CS(m)-SeNPs, CS(h)-SeNP were about 1.314, 1.249, 1.143 and 1.101 mM. Based on these results, our strategy to decorate the CS(h) on SeNPs exhibited a higher $ABTS^{\bullet+}$ scavenging activity than CS(l)-SeNPs, and was similar with CS(m)-SeNPs.

3.7 Superoxide anion radical scavenging ability

Superoxide anion is an oxygen-centred radical with low reactive ability. However, it plays an important role in investigating the antioxidant activities due to that it can cause oxidative damage in human body, inducing damage in DNA, protein and lipids through accelerating the formation of other ROS [28]. As can be seen in Fig. 6*c*, SeNPs and CS coated SeNPs exhibited stronger $O_2^{\bullet-}$ scavenging effect in a concentration-dependent manner. The percentage inhibition of superoxide anion radical generation by 1 mM concentration of SeNPs was found as 15.58%. On the other hand, at the same concentration, CS(l)-SeNPs, CS(m)-SeNPs, CS(h)-SeNPs exhibited 25.20, 27.54, 31.44% superoxide anion radical scavenging activity, respectively. More importantly, CS(h)-

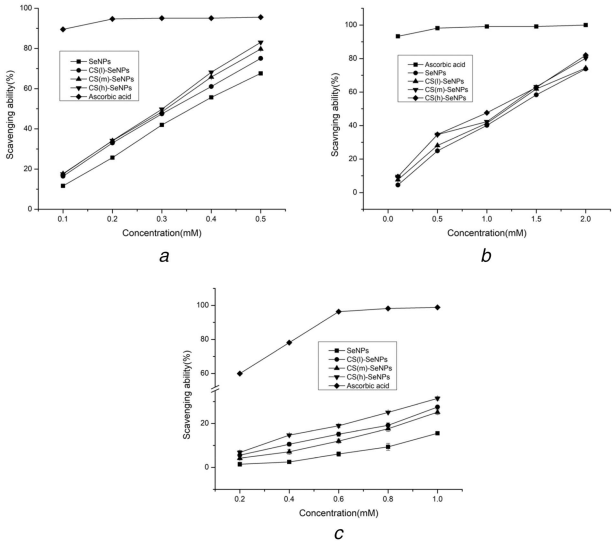

Fig. 6 *Scavenging ability of SeNPs, CS(l)-SeNPs, CS(m)-SeNPs, CS(h)-SeNPs towards*

(a) DPPH radicals, ***(b)*** ABTS radicals, ***(c)*** $O_2^{\bullet-}$ radicals

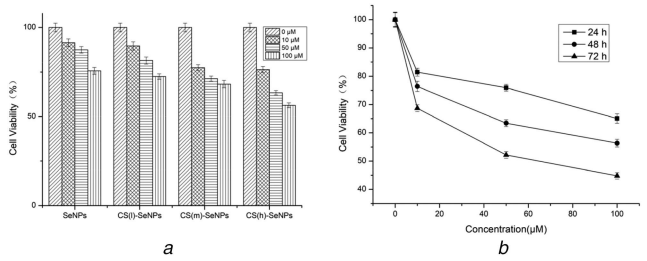

Fig. 7 *The Cytotoxicity assay determined by WST-1*

(a) Growth inhibition of SeNPs, CS(l)-SeNPs, CS(m)-SeNPs and CS(h)-SeNPs against HepG2 cancer cell for 48 h, ***(b)*** Cell viability after treatment with different concentrations of CS(h)-SeNPs for 24, 48 and 72 h

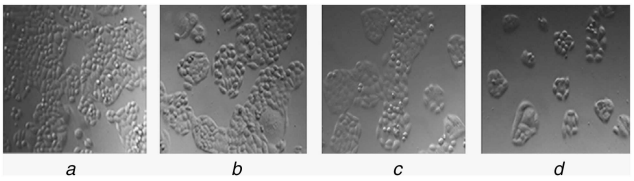

Fig. 8 *Morphological assessment of the anticancer effect of CS(h)-SeNPs against HepG2 cancer cell line after 48 h incubation visualised under an inverted phase-contrast microscope at 40 × magnification*

(a) Control (untreated) cells, ***(b)*** 10 μM SeNPs treated cells, ***(c)***10 μM CS(h)-SeNPs treated cells, ***(d)*** 100 μM CS(h)-SeNPs treated cells for 48 h

SeNPs showed higher $O_2^{\bullet-}$ scavenging effect than CS(l)-SeNPs and CS(m)-SeNPs. It may be considered that the chain density of low MW of CS is too low to fully and closely cover the outer surface of SeNPs, which affect the interaction between the CS and SeNPs, resulting in weak antioxidant activities. The results showed that SeNPs coated with different Mw CS can enhance the antioxidant activity in vitro compared to the undecorated SeNPs.

3.8 Cytotoxicity assay

As shown in Fig. 7*a*, CS(h)-SeNPs at concentrations of 10, 50 and 100 mM (with the same concentration of 0.08 mg/ml CS) significantly decreased the cell viability to 76.63, 63.31 and 56.34% of control group, respectively. However, under the corresponding conditions, SeNPs at the same concentrations only slightly decreased the cell viability to 91.49, 87.46 and 75.69%. SeNPs decorated with different MW of CS exhibited higher cytotoxicity towards HepG2 compared to SeNPs, which demonstrated that the CS decorated on the surface of SeNPs significantly enhanced the anticancer activity. Moreover, the cytotoxicity of CS(m)-SeNPs was lower than CS(h)-SeNPs and higher than CS(l)-SeNPs. It was well known that the formation of reactive oxygen species or increase in intracellular oxidative stress may consider as the plausible mechanism for the anticancer effect of nanocomposites [29]. As shown above, CS(h)-SeNPs had higher antioxidant activities than CS(m)-SeNPs and CS(l)-SeNPs, which was corresponding with the results of cytotoxicity assay. Fig. 7*b* shows that the treatments of CS(h)-SeNPs inhibited the growth of HepG2 cells in a time- and dose-dependent manner. As shown in Fig. 8, the typical morphological assessment of cells revealed that the treatment of CS(h)-SeNPs on HepG2 cells reduced cell density by altering cellular morphology when compared to that of untreated cells (control) and with the increased concentration, the cell density decreased. The results directly indicated a pronounced cytotoxic effect of CS-SeNPs on HepG2 cells, which showed a potential application in cancer chemoprevention. As shown above, CS(h)-SeNPs had higher antioxidant activities than CS(m)-SeNPs and CS(l)-SeNPs, which was corresponding with the results of cytotoxicity assay.

4 Conclusion

A green method for synthesis SeNPs was investigated in this work, and then decorated with different MW of CS to obtain CS(l)-SeNPs, CS(m)-SeNPs and CS(h)-SeNPs, respectively. The results showed that the addition of CS do not affect the morphology of SeNPs, and can keep it stable for at least one month, which is due to the C–O–Se bonds generated by the strong interactions between the OH groups of CS and SeNPs. Moreover, compared to SeNPs, the decoration of different MW CS on SeNPs enhanced the DPPH, $ABTS^{\bullet+}$ and superoxide anion radicals scavenging ability, and CS(h)-SeNPs were more stable and exhibited the highest scavenging ability towards DPPH, $O_2^{\bullet-}$ and $ABTS^{\bullet+}$ radicals and also significantly enhanced the cytotoxicity of SeNPs towards HepG2 cancer cells. This work revealed the structure-property relationship between SeNPs and surface decorated agent and proved that surface chemistry played an important role in stability, antioxidant and anticancer properties of SeNPs, providing a design element for prediction and rational design of new antioxidant.

5 Acknowledgments

This work was financially supported by the National Natural Science Foundation of China (grant no. 31700709), the Natural Science Foundation of Jiangsu Province (BK20160170), the program of Collaborative Innovation Center of Food Safety and Quality Control in Jiangsu Province, the program of 2014 Taishan Talents Team Scholar Blue Industry.

6 References

[1] Dutta, P.K., Tripathi, S., Mehrotra, G.K., *et al.*: 'Perspectives for chitosan based antimicrobial films in food applications', *Food Chem.*, 2009, **114**, (4), pp. 1173–1182

[2] Thakor, A.S., Gambhir, S.S.: 'Nanooncology: the future of cancer diagnosis and therapy', *CA-Cancer J. Clin.*, 2013, **63**, (6), pp. 395–418

[3] McClements, J., McClements, D.J.: 'Standardization of nanoparticle characterization: methods for testing properties, stability, and functionality of edible nanoparticles', *Crit. Rev. Food Sci. Nutr.*, 2016, **56**, (8), pp. 1334–1362

[4] Thomson, C.D.: 'Assessment of requirements for selenium and adequacy of selenium status: a review', *Eur. J. Clin. Nutr.*, 2004, **58**, (3), pp. 391–402

[5] Maiyo, F., Singh, M.: 'Selenium nanoparticles: potential in cancer gene and drug delivery', *Nanomedicine*, 2017, **12**, (9), pp. 1075–1089

[6] Gallego-Gallegos, M., Doig, L.E., Tse, J.J., *et al.*: 'Bioavailability, toxicity and biotransformation of selenium in midge (Chironomus Dilutus) larvae exposed via water or diet to elemental selenium particles, selenite, or selenized algae', *Environ. Sci. Technol.*, 2013, **47**, (1), pp. 584–592

[7] Kokila, K., Elavarasan, N., Sujatha, V.: 'Diospyros montana leaf extract-mediated synthesis of selenium nanoparticles and their biological applications', *New J. Chem.*, 2017, **41**, (15), pp. 7481–7490

[8] Xiao, Y.D., Huang, Q.L., Zheng, Z.M., *et al.*: 'Construction of a cordyceps sinensis exopolysaccharide-conjugated selenium nanoparticles and enhancement of their antioxidant activities', *Int. J. Biol. Macromol.*, 2017, **99**, pp. 483–491

[9] Guisbiers, G., Lara, H.H., Mendoza-Cruz, R., *et al.*: 'Inhibition of candida albicans biofilm by pure selenium nanoparticles synthesized by pulsed laser ablation in liquids', *Nanomed. Nanotechnol. Biol. Med.*, 2017, **13**, (3), pp. 1095–1103

[10] Zhu, C.H., Zhang, S.M., Song, C.W., *et al.*: 'Selenium nanoparticles decorated with ulva lactuca polysaccharide potentially attenuate colitis by inhibiting Nf-kappa B mediated hyper inflammation', *J. Nanobiotechnol.*, 2017, **15**, (20), pp. 1–15
[11] Pi, J., Jin, H., Liu, R.Y., *et al.*: 'Pathway of cytotoxicity induced by folic acid modified selenium nanoparticles in Mcf-7 cells', *Appl. Microbiol. Biotechnol.*, 2013, **97**, (3), pp. 1051–1062
[12] Wu, H.L., Zhu, H.L., Li, X.L., *et al.*: 'Induction of apoptosis and cell cycle arrest in A549 human lung adenocarcinoma cells by surface-capping selenium nanoparticles: an effect enhanced by polysaccharide-protein complexes from polyporus rhinocerus', *J. Agric. Food Chem.*, 2013, **61**, (41), pp. 9859–9866
[13] Wu, H.L., Li, X.L., Liu, W., *et al.*: 'Surface decoration of selenium nanoparticles by mushroom polysaccharides-protein complexes to achieve enhanced cellular uptake and antiproliferative activity', *J. Mater. Chem.*, 2012, **22**, (19), pp. 9602–9610
[14] Yu, B., Zhang, Y.B., Zheng, W.J., *et al.*: 'Positive surface charge enhances selective cellular uptake and anticancer efficacy of selenium nanoparticles', *Inorg. Chem.*, 2012, **51**, (16), pp. 8956–8963
[15] Zhang, C., Zhai, X., Zhao, G., *et al.*: 'Synthesis, characterization, and controlled release of selenium nanoparticles stabilized by chitosan of different molecular weights', *Carbohydr. Polym.*, 2015, **134**, pp. 158–166
[16] Zhai, X., Zhang, C., Zhao, G., *et al.*: 'Antioxidant capacities of the selenium nanoparticles stabilized by chitosan', *J. Nanobiotechnology*, 2017, **15**, (1), pp. 1–12
[17] Ng, C.H.B., Fan, W.Y.: 'Colloidal beading: sonication-induced stringing of selenium particles', *Langmuir*, 2014, **30**, (25), pp. 7313–7318
[18] Yamaguchi, T., Takamura, H., Matoba, T., *et al.*: 'Hplc method for evaluation of the free radical-scavenging activity of foods by using 1,1-diphenyl-2-picrylhydrazyl', *Biosci. Biotechnol., Biochem.*, 1998, **62**, (6), pp. 1201–1204
[19] Arnao, M.B., Cano, A., Acosta, M.: 'The hydrophilic and lipophilic contribution to total antioxidant activity', *Food Chem.*, 2001, **73**, (2), pp. 239–244
[20] Tamburaci, S., Tihminlioglu, F.: 'Diatomite reinforced chitosan composite membrane as potential scaffold for guided bone regeneration', *Mater. Sci. Eng. C, Mater. Biol. Appl.*, 2017, **80**, pp. 222–231
[21] Ng, C.H.B., Fan, W.Y.: 'Facile synthesis of single-crystalline gamma-Cui nanotetrahedrons and their induced transformation to tetrahedral Cuo nanocages', *J. Phys. Chem. C*, 2007, **111**, (26), pp. 9166–9171
[22] Abbasi, A.R., Morsali, A.: 'Syntheses and characterization of Agi nano-structures by ultrasonic method: different morphologies under different conditions', *Ultrason. Sonochem.*, 2010, **17**, (3), pp. 572–578
[23] Molina, R., Al-Salama, Y., Jurkschat, K., *et al.*: 'Potential environmental influence of amino acids on the behavior of Zno nanoparticles', *Chemosphere*, 2011, **83**, (4), pp. 545–551
[24] Siripatrawan, U., Harte, B.R.: 'Physical properties and antioxidant activity of an active film from chitosan incorporated with green tea extract', *Food Hydrocolloids*, 2010, **24**, (8), pp. 770–775
[25] Huang, B., Zhang, J.S., Hou, J.W., *et al.*: 'Free radical scavenging efficiency of nano-Se in vitro', *Free Radical Biol. Med.*, 2003, **35**, (7), pp. 805–813
[26] Forootanfar, H., Adeli-Sardou, M., Nikkhoo, M., *et al.*: 'Antioxidant and cytotoxic effect of biologically synthesized selenium nanoparticles in comparison to selenium dioxide', *J. Trace Elem. Med. Biol.*, 2014, **28**, (1), pp. 75–79
[27] Re, R., Pellegrini, N., Proteggente, A., *et al.*: 'Antioxidant activity applying an improved abts radical cation decolorization assay', *Free Radical Biol. Med.*, 1999, **26**, (9–10), pp. 1231–1237
[28] Masek, A., Chrzescijanska, E., Latos, M.: 'Determination of antioxidant activity of caffeic acid and P-coumaric acid by using electrochemical and spectrophotometric assays', *Int. J. Electrochem. Sci.*, 2016, **11**, (12), pp. 10644–10658
[29] Arjunan, N., Kurnari, H.L.J., Singaravelu, C.M., *et al.*: 'Physicochemical investigations of biogenic chitosan-silver nanocomposite as antimicrobial and anticancer agent', *Int. J. Biol. Macromol.*, 2016, **92**, pp. 77–87